

Accepted Manuscript

New SrPb₃Br₈ crystals: Growth, crystal structure and optical properties

Ludmila I. Isaenko, Alina A. Goloshumova, Alexander P. Yelisseyev, Yuri V. Shubin, O.Y. Khyzhun, Dmitrii Yu. Naumov, Alexandra Yu. Tarasova



PII: S0925-8388(16)31343-3

DOI: [10.1016/j.jallcom.2016.05.024](https://doi.org/10.1016/j.jallcom.2016.05.024)

Reference: JALCOM 37542

To appear in: *Journal of Alloys and Compounds*

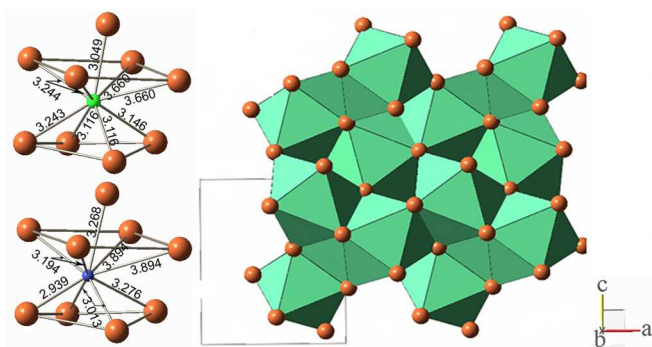
Received Date: 19 January 2016

Revised Date: 21 April 2016

Accepted Date: 3 May 2016

Please cite this article as: L.I. Isaenko, A.A. Goloshumova, A.P. Yelisseyev, Y.V. Shubin, O.Y. Khyzhun, D.Y. Naumov, A.Y. Tarasova, New SrPb₃Br₈ crystals: Growth, crystal structure and optical properties, *Journal of Alloys and Compounds* (2016), doi: 10.1016/j.jallcom.2016.05.024.

This is a PDF file of an unedited manuscript that has been accepted for publication. As a service to our customers we are providing this early version of the manuscript. The manuscript will undergo copyediting, typesetting, and review of the resulting proof before it is published in its final form. Please note that during the production process errors may be discovered which could affect the content, and all legal disclaimers that apply to the journal pertain.



New SrPb₃Br₈ crystals: growth, crystal structure and optical properties

Ludmila I. Isaenko^{1,2}, Alina A. Goloshumova^{1,*}, Alexander P. Yelisseyev¹, Yuri V. Shubin^{2,3}, O.Y. Khyzhun⁴, Dmitrii Yu. Naumov³, Alexandra Yu. Tarasova¹

¹V.S. Sobolev Institute of Geology and Mineralogy of Siberian Branch of Russian Academy of Sciences, 43, Russkaya Street, Novosibirsk, 630058, Russia

²Novosibirsk State University, 2, Pirogova Street, Novosibirsk, 630090, Russia

³Nikolaev Institute of Inorganic Chemistry Siberian Branch of Russian Academy of Sciences, 3, Acad. Lavrentiev Ave., Novosibirsk, 630090, Russia

⁴ Frantsevych Institute for Problems of Materials Science, National Academy of Sciences of Ukraine, 3 Krzhizhanivsky Street, UA-03142 Kyiv, Ukraine

Abstract

SrBr₂ - PbBr₂ system was investigated. A new compound of SrPb₃Br₈ was obtained and investigated by powder and single crystal XRD and spectroscopic methods. SrPb₃Br₈ crystals have orthorhombic symmetry with *Pnma* space group, $a = 8.0056(4)$ Å, $b = 4.7359(2)$ Å, $c = 9.5208(5)$ Å. These crystals are transparent from ≈ 360 nm, the band gap is 3.20 eV and calculated density is 6.242 g/cm³. Electronic structure of SrPb₃Br₈ was elucidated based on data

of X-ray photoelectron spectroscopy (XPS) and X-ray emission spectroscopy (XES). In particular, XPS core-level and valence-band spectra were measured for pristine and Ar⁺ ion-irradiated surfaces of SrPb₃Br₈ crystals. The XPS results reveal high hygroscopicity of the SrPb₃Br₈ single crystal surface. Comparison on a common energy scale of the XPS valence-band spectrum of SrPb₃Br₈ the XES Br Kβ₂ band representing the energy distribution of the Br 4p states in this bromide indicate that the principle contributions of the Br 4p states occur in the upper portion of the valence band, with also their significant contributions in other valence-band portions.

Keywords

A. Inorganic materials; B. Crystal growth; C. Crystal structure; C. Optical properties; D. X-ray diffraction; D. Photoelectron spectroscopies

1. Introduction

An intense search for new active media for solid state lasers generating in mid-infrared range revealed a family of double halogenides of alkali metals APb₂Br₅, where A=K, Rb. The cycle of works on obtaining of this group of crystals was initiated 15 years ago. As a result crystals with a unique set of properties were developed [1]. These compounds appeared to be chemically stable and transparent in a wide range (0.35-30 μm). They have a low-energy phonon spectrum which results in minimum heat losses and high quantum yield of the radiative processes. The conditions of the matrix effective doping with rare-earth elements were found and a group of crystals promising as laser media for visible and infrared ranges was created [2-5]. RbPb₂Br₅ (RPB) and KPb₂Br₅ (KPB) crystals have a density of 5.62 and 5.83 g/cm³, respectively. Loose packing of the ions with large radius provides comprehensive facilities for variation of crystals composition

and properties and opens prospects for their use not only as active laser matrices, but also as promising scintillation materials. High density and the possibility of crystal doping with rare-earth ions are important characteristics of effective scintillation crystal. Scintillation crystals are now an important part of many applications, including the detection of gamma radiation with high energy resolution to identify isotopes. Many research works are devoted to obtain effective stable material with optimal scintillation properties (high energy resolution, light yield, etc.). There are some specific requirements for gamma spectroscopy, such as a high atomic number (which provides a good stopping power for gamma rays) and the absence of natural radioactivity [6]. Strontium ions are easily replaced with rare-earth ions in crystal lattices because of the similarity in their ionic radii. Therefore replacing of alkali ions (K and Rb) with strontium in the matrices of listed bromides is considered as the way to obtain a new potential scintillation material. The $\text{SrBr}_2\text{-PbBr}_2$ system was not studied to date and there are no data in literature. In the present work new SrPb_3Br_8 crystal was grown for the first time, its crystal structure and some spectroscopic properties were investigated. In particular, X-ray photoelectron spectroscopy (XPS) and X-ray emission spectroscopy (XES) were used in the present work to measure the XPS core-level and valence-band spectra as well as the XES Br $K\beta_2$ band (Br 4p states) of the SrPb_3Br_8 crystal.

2. Experimental details

To obtain crystals of ternary compounds SrBr_2 and PbBr_2 were used as initial materials. Binary bromides were prepared by dissolving SrCO_3 (99.99%) and pre-purified $\text{Pb}(\text{NO}_3)_2$ in hydrobromic acid HBr (99.99%). For further purification synthesized bromides were subjected to the repeated directed crystallization with a preliminary removal of contaminated parts. The purified components were placed in a quartz ampoule, which then was evacuated, sealed and

placed in a horizontal furnace. Then the mixture was melted at the temperature of 380°C and stirred up during 24 hours for complete composition homogenization. The resulting material was loaded into a quartz growth container. Crystals were grown by the vertical Bridgman method. The vertical temperature gradient in the growth zone was about 20°/cm, the speed of the ampoule lowering into the cold zone was 2-5 mm/day. As a result sufficiently pure and transparent crystal boule up to $\varnothing 15 \times 100$ mm in size was obtained (Fig. 1). Crystal boule is homogeneous, but in its middle part there are turbid blocks several millimeters in size.

To determine phase composition of obtained boules the powder X-Ray diffraction analysis was used. Samples were cut from conic, middle and end parts of the crystal boule and then were grinded to dispersed powders. The PXRD analysis of the samples was performed at room temperature on a Shimadzu XRD-7000 diffractometer (CuK α radiation, Ni filter on the reflected beam, scintillation detector with amplitude discrimination). The patterns were recorded in the step mode in the angular range $2\theta = 10-85^\circ$, with a step 0.05. The phase nature of the prepared compound was determined by indexing the powder diffraction patterns of the complexes using the single crystal XRD data. Indexing of the diffraction patterns for the products of hydrolysis was carried out using the data reported in the PDF database [7]. Unit cell parameters were refined by the full-profile technique within the whole diffraction range using the PowderCell 2.4 software [8].

Clean and optically transparent sample $0.13 \times 0.07 \times 0.02$ mm³ in size was cut from the middle part of the grown boule and used for single crystal XRD experiment. Single crystal data were collected with the MoK α -radiation using a Bruker APEX DUO diffractometer equipped with a graphite monochromator. All calculations were performed using SHELXTL software {Bruker AXS Inc. (2004), APEX (Version 1.08), SAINT (Version 7.03), SADABS (Version 2.11) и

SHELXTL (Version 6.12) Bruker Advanced X-Ray Solutions – Madison, Wisconsin, USA}.

Coordination numbers of cations in studied structures were defined by the Dirichlet polyhedra method using the Xshell software [9]. For graphic visualization the BS program (Balls & Sticks ver. 1.42 by Sung J. Kang & Tadashi C. Ozawa) was used.

Transmission spectra were recorded at 300 K in the UV to near IR and mid-IR spectral ranges using a Shimadzu PC-2501 and a Fourier-transform Infracum FT-801 spectrometers, respectively. Plates of SrPb_3Br_8 and PbBr_2 300 and 60 microns thick, respectively, with cleaved natural faces were used for these measurements. Absorption spectra were then calculated taking into account the multiple reflections from the opposite parallel flat faces of the plates. We analyzed the so called Tauc plot of $(\alpha h\nu)^n$ vs $h\nu$ in the region of the short-wavelength edge of the transparency region, where α is the absorption coefficient deduced from the transmission data and $h\nu$ is the photon energy. The index of power (n) for the Tauc plot determines the type of the band-to-band electron transitions [10].

Features of the electronic structure of the SrPb_3Br_8 crystal were clarified based on XPS and XES measurements. The XPS core-level and valence-band spectra of SrPb_3Br_8 were measured using the UHV-Analysis-System produced by SPECS Surface Nano Analysis Company (Berlin, Germany). The System is equipped with a hemispherical PHOIBOS 150 analyzer and the XPS spectra were recorded in an ion-pumped chamber at a base pressure less than 7×10^{-10} mbar. The XPS spectra were excited by a Mg $K\alpha$ source of X-ray radiation ($E=1253.6$ eV) were attained at a constant pass energy of 35 eV. The spectrometer energy scale was calibrated following the technique reported in detail in [5]. The C 1s line (284.6 eV) of adventitious carbon was used as a reference to account for the charging effects as it is offered for ternary lead-bearing bromides

[11, 12]. To remove surface contaminations, we have performed the bombardment of SrPb_3Br_8 single crystal surface by Ar^+ ions with the energy of 3.0 keV over 5 min at the ion current density of $17 \mu\text{A}/\text{cm}^2$ (a total Ar^+ flux was estimated to be $\sim 5.3 \times 10^{16}$ ions/ cm^2). This method of surface cleaning is the same used earlier for a number of ternary lead-containing bromides [5, 11, 12]. In addition, following the experimental studies and first-principles band-structure calculations of ternary Pb-bearing bromides indicating that their electronic structures are defined by significant contributions of the Br 4p states throughout the whole valence band region [11-14], we have also measured XES Br $\text{K}\beta_2$ band ($\text{K} \rightarrow \text{M}_{\text{II,III}}$ transition) that represents peculiarities of the energy distribution of the valence Br p states. In the present work, the XES Br $\text{K}\beta_2$ band was recorded with energy resolution of about 0.3 eV employing a Johann-type DRS-2M spectrograph equipped with an X-ray BHV-7 tube (gold anode) operating at accelerating voltage, $U_a = 45.0$ kV, and anode current, $I_a = 72.5$ mA. The disperse element was a quartz crystal with the (0001) reflecting plane.

3. Results and discussion

The results of powder x-ray phase analysis are shown at Fig. 2. There is one main phase on diffraction patterns of all three samples. Its peaks correspond to the reference diffraction pattern of lead bromide, but their position is shifted towards smaller angles. This indicates an increase of unit cell parameters in comparison with the structure of pure lead bromide. In more detail, this phase was studied by single crystal x-ray diffraction analysis. Besides there are additional weak peaks attributable to other unidentified phase on the diffraction pattern of the sample made from the middle part of crystal boule (Fig. 2, \blacklozenge). Low intensity of peaks indicates its low content of about 20% in the sample.

According to powder X-Ray diffraction results crystal structure of the main phase is rather similar to lead bromide. To estimate the difference between them X-Ray diffraction analysis was carried out for PbBr_2 and crystals of obtained compound. The results and structure refinement data are given in Table 1.

Single crystal X-Ray diffraction analysis showed that obtained compound is SrPb_3Br_8 crystal of orthorhombic system with Pnma space group. Strontium and lead ions each have one nonequivalent position in crystal structure, bromine ions have two positions. As a result of Dirichlet polyhedra constructing it was found that the coordination number of cations is 9. Table 2 shows cation-anion bond lengths in SrPb_3Br_8 crystal in comparison with similar characteristics for PbBr_2 crystal. According to bond lengths two coordination spheres for each cation can be selected. The first one is formed by seven bromine ions, and the second coordination sphere includes another two Br^- ions. Coordination polyhedra of Sr^{2+} and Pb^{2+} cations are monocapped tetragonal prisms.

SrPb_3Br_8 crystal structure is slightly changed crystal structure of PbBr_2 , where part of lead ions is substituted by Sr^{2+} ions (Fig. 3). In this case lead coordination polyhedra, which are occupied by strontium, become distorted, cation-anion bond lengths for Sr^{2+} and Pb^{2+} ions are different (Table 2).

The positions of both cations differ from Pb^{2+} ion position in pure lead bromide structure: as opposed to the latter in the structure of ternary compound Sr^{2+} and Pb^{2+} are slightly displaced, therefore SrPb_3Br_8 lattice is slightly distorted in comparison with PbBr_2 (Fig. 4).

On the basis of single crystal x-ray diffraction data the diffraction pattern for SrPb_3Br_8 crystal was calculated (Fig. 2, SrPb_3Br_8). It corresponds completely to the main phase on the diffraction

patterns obtained by powder x-ray analysis. This confirms that the main phase in the obtained crystal boule conforms SrPb_3Br_8 .

Transmission spectra were recorded for thin SrPb_3Br_8 and PbBr_2 plates, which were 300 and 60 μm thick, respectively (Fig. 5). and absorption spectra were calculated on their basis. Both crystals become transparent from $\approx 0.36 \mu\text{m}$ and they stay transparent up to 20 μm at least. For SrPb_3Br_8 the transparency grows smoothly as wavelength increases up to 1.5 μm whereas at longer wavelengths one can see some structure: broad bands near 2.5 and 15 μm and narrow lines at 2.89, 6.26 and 8.05 μm . According to Tennison et al [15] these lines in the mid-IR are associated with water molecules and O-H vibrations (Table 3). Strong absorption at about 2.89 μm is caused by stretch vibrations in H_2O molecules and OH groups. Absorption features at 6.26 μm and 15 μm correspond to ν_2 , bend vibrations and L_2 librations in H_2O , respectively. Origin of the 8.05 μm absorption line is not clear to date.

A Tauc plot [16] was used to determine the optical bandgap. Unfortunately the absorption spectra both for SrPb_3Br_8 and PbBr_2 did not show a flattening in the coordinates of $(\alpha \times hv)^2 = f(hv)$ or $(\alpha \times hv)^{0.5} = f(hv)$ as was expected for the cases of direct or indirect band-to-band electronic transitions, respectively. However, we found that the absorption dependence versus photon energy was close to an exponential one (Fig. 6). Following F. Urbach [17, 18] such shape of the $\alpha(hv)$ spectrum typically is associated with electronic transitions from the valence to conduction band tail in disordered solids. It is necessary to note that a shortwave absorption edge is located near 3.2 eV for PbBr_2 , which is considerably lower than the $E_g = 4.2$ eV value, obtained from the reflection and luminescence excitation spectra [19, 20]. A possible reason of such difference may be an intense band of excitonic absorption, located near 3.95 eV in PbBr_2 [19, 20]. Similar situation takes place in SrMgF_4 single crystal: absorption edge is near 10.5 eV

whereas $E_g = 12.5$ eV according to results of reflection and luminescence excitation spectroscopy [21, 22]. Taking into account close values for shortwave absorption edge for SrPb_3Br_8 and PbBr_2 single crystals (Fig. 5), we expect that bandgap values for these crystals are also similar (about 4.2 eV from [19, 20]).

Thus, spectroscopic studies indicate the presence of impurities of oxygen-containing compounds. Strontium-containing halides are highly hygroscopic [23, 24], therefore oxygen-containing compounds could be formed at the stage of synthesis or sample preparation. Considering the composition of the starting components in the system, it can be assumed that the detected second phase of unidentified composition is an oxygen-containing compound of strontium.

The above suggestions are confirmed by the present XPS results. Fig. 7 presents the survey XPS spectra of both pristine and Ar^+ ion-bombarded surfaces of the studied SrPb_3Br_8 crystal. From the figure, it is apparent that all the features of the survey XPS spectra, except of carbon and oxygen 1s levels and KLL Auger lines, are attributed to the core-levels of atoms constituting the SrPb_3Br_8 compound. As one can see from Fig. 7, relative intensities of the XPS O 1s and C 1s core-level lines are rather high on the pristine surface of the SrPb_3Br_8 crystal to adsorbed oxygen-containing species, hydrocarbons and water. Further, as Fig. 8a presents, the maximum of the XPS Pb $4f_{7/2}$ core-level spectrum is detected on the pristine SrPb_3Br_8 crystal surface at the binding energy of about 138.9 eV. This fact indicates that lead atoms on the pristine SrPb_3Br_8 surface are mainly in the formal valence +3 [25-27]. Figs. 7 and 8 reveal that the surface treatment with 3.0 keV Ar^+ ions over 5 min at ion current density fixed at $14 \mu\text{A}/\text{cm}^2$ causes decreasing relative intensities of the XPS C 1s and O 1s lines as well as relative content of Pb^{3+} ions in the topmost SrPb_3Br_8 crystal layers. As a result of such a bombardment, the relative

contents of Pb^{2+} and Pb^{3+} ions become comparative (see Fig. 8a). However, the Ar^+ ion-bombardment do not alter charge states of Sr and Br atoms because the binding energies of the XPS Br $3p_{3/2}$ and Sr $3p_{3/2}$ core-level spectra do not change within the accuracy of the present measurements, namely ± 0.1 eV (Figs. 8b and 8c). Fig. 9 shows that the mentioned Ar^+ irradiation does not cause significant changes of the energy distribution of the electronic states within the valence band region as well. As can be seen from Fig. 9, the Ar^+ ion-bombardment makes visible two fine-structure peculiarities A and B of the XPS valence-band spectrum that are not resolved on the spectrum of the pristine surface of the SrPb_3Br_8 crystal. It is worth mentioning that the SrPb_3Br_8 compound looks to be very different from other ternary lead-bearing bromides, namely Tl_3PbBr_5 and APb_2Br_5 ($A = \text{K, Rb, Tl}$), which were proved to possess very low hygroscopicity [11-14, 28].

Results of comparison of the X-ray emission Br $\text{K}\beta_2$ band and the XPS valence-band spectrum of SrPb_3Br_8 provided that a common energy scale is used are plotted in Fig. 10. The technique of matching the above X-ray spectra of the SrPb_3Br_8 crystal on a common energy scale is similar to that used earlier for a number of ternary lead-contained bromides (see, e.g. Refs. [13, 14]), and it is generally used in experimental studies of solids using the XPS and XES method [29]. The experimental XPS and XES results depicted in Fig. 10 show that the principal contributions of the Br 4p states occur in the upper portion of the valence band, with also significant contributions of the valence Br p states throughout the whole valence band region of SrPb_3Br_8 . Similar conclusion was made when studying the electronic structure of a number of ternary lead-bearing bromides Tl_3PbBr_5 and APb_2Br_5 ($A = \text{K, Rb, Tl}$) [11-14, 28]. Regrettably, available facilities do not allow measurements of the energy distribution of the valence s and p

states associated with lead and strontium atoms that are expected to be the other contributors to the valence band of the SrPb_3Br_8 compound.

4. Conclusions

Ternary compound of SrPb_3Br_8 composition is crystallized in SrBr_2 - PbBr_2 system. SrPb_3Br_8 crystal structure has Pnma symmetry, $a = 8.0056(4) \text{ \AA}$, $b = 4.7359(2) \text{ \AA}$, $c = 9.5208(5) \text{ \AA}$. These crystals are transparent from $\approx 360 \text{ nm}$, bandgap is estimated as 3.20 eV . Calculated density is 6.242 g/cm^3 and allows one to consider the SrPb_3Br_8 crystals as a potential scintillation material. The present XPS results indicate that all features of the survey spectra of SrPb_3Br_8 , except of carbon and oxygen $1s$ levels and KLL Auger lines, are attributed to the core-levels of atoms constituting the compound under consideration. Further, the XPS measurements indicate that the SrPb_3Br_8 crystal surface is highly hygroscopic. Matching the XPS valence-band spectrum on a common energy scale with the X-ray emission $\text{Br K}\beta_2$ band, which represents the energy distribution of the $\text{Br } 4p$ states, allows for concluding that the $\text{Br } 4p$ states contribute mainly in the upper portion of the valence band of SrPb_3Br_8 , with also their significant contributions in other valence-band portions. The study of SrBr_2 - PbBr_2 system will be continued.

Acknowledgements

This work is supported by Russian Foundation of Basic Research (grant № 16-32-00545). Authors thank V.M. Pashkov for help with crystal growth.

AUTHOR INFORMATION

Corresponding Author

*Phone/Fax: +7 383 306 63 88. E-mail: alingol-nsk@yandex.ru

REFERENCES

- [1] M.C. Nostrand, R.H. Page, W.F. Payne, W.F. Krupke, S. Schunemann, L.I. Isaenko, Spectroscopic data infrared transitions in $\text{CaGa}_2\text{S}_4:\text{Dy}^{3+}$ and $\text{KPb}_2\text{Cl}_5:\text{Dy}^{3+}$, ASSL TOPS XIX, Washington, D.C., 1998, p 524.
- [2] L.I. Isaenko, A.A. Merkulov, S.V. Melnikova, V.M. Pashkov, A.Yu. Tarasova, Effect of K \leftrightarrow Rb Substitution on Structure and Phase Transition in Mixed $\text{K}_x\text{Rb}_{1-x}\text{Pb}_2\text{Br}_5$, Cryst. Growth Des. 9 (2009) 2248–2251.
- [3] I.N. Ogorodnikov, A.A. Smirnov, V.A. Pustovarov, L.I. Isaenko, A.Y. Tarasova, V.Y. Yakovlev, Transient optical absorption and luminescence in APb_2Cl_5 (A = K, Rb) crystals, Phys. Solid State. 51 (2009) 1640-1648.
- [4] A.Yu. Tarasova, Yu.V. Seryotkin, V.M. Pashkov, L.I. Isaenko, Coefficients of thermal expansion of KPb_2Cl_5 and RbPb_2Br_5 crystals, JTAC. 104 (2011) 795-796.
- [5] A.Yu. Tarasova, L.I. Isaenko, V.G. Kesler, V.M. Pashkov, N.M. Denysyuk, O.Yu. Khyzhun, A.P. Yelisseyev, Electronic structure and fundamental absorption edges of KPb_2Br_5 , $\text{K}_{0.5}\text{Rb}_{0.5}\text{Pb}_2\text{Br}_5$ and RbPb_2Br_5 single crystals, J. Phys. Chem. Solids. 73 (2012) 674-682.
- [6] E.D. Bourret-Courchesne, G.A. Bizarri, R. Borade, G. Gundiah, E.C. Samulon, Z. Yan, S.E. Derenzo, Crystal growth and characterization of alkali-earth halide scintillators, J. Cryst. Growth 352 (2012) 78 – 83.
- [7] Powder Diffraction File, PDF-2/Release 2009, 2009: International Centre for Diffraction Date, USA.
- [8] G. Nolze, W. Kraus, Powder Diffr. 13 (1998) 25.

- [9] N.E. Kashcheeva, D.Y. Naumov, E.V. Boldyreva, Software for calculating Dirichlet domains and examples of its application for the analysis of crystal structures of cobalt(III)nitropentaammines, *Z. Kristallogr.* 214 (1999) 534 – 541.
- [10] D.L. Wood, J. Tauc, Weak absorption tails in amorphous semiconductors, *Phys. Rev. B.* 5 (1972) 3144 – 3151.
- [11] O.Y. Khyzhun, V.L. Bekenev, O.V. Parasyuk, S.P. Danylchuk, N.M. Denysyuk, A.O. Fedorchuk, N. AlZayed, I.V. Kityk, Single crystal growth and the electronic structure of orthorhombic Tl_3PbBr_5 : A novel material for non-linear optics, *Opt. Mater.* 35 (2013) 1081–1089.
- [12] O.Y. Khyzhun, V.L. Bekenev, N.M. Denysyuk, I.V. Kityk, P. Rakus, A.O. Fedorchuk, S.P. Danylchuk, O.V. Parasyuk, Single crystal growth and the electronic structure of $TlPb_2Br_5$, *Opt. Mater.* 36 (2013) 251–258.
- [13] A.A. Lavrentyev, B.V. Gabrelian, V.T. Vu, N.M. Denysyuk, P.N. Shkumat, A.Y. Tarasova, L.I. Isaenko, O.Y. Khyzhun, Electronic structure and optical properties of $RbPb_2Br_5$, *J. Phys. Chem. Solids.* 91 (2016) 25–33.
- [14] A.A. Lavrentyev, B.V. Gabrelian, V.T. Vu, N.M. Denysyuk, P.N. Shkumat, A.Y. Tarasova, L.I. Isaenko, O.Y. Khyzhun, Specific features of the electronic structure and optical properties of KPb_2Br_5 : DFT calculations and X-ray spectroscopy measurements, *Opt. Mater.* 53 (2016) 64–72.
- [15] J. Tennyson, P.F. Bernath, L.R. Brown, A. Campargue, A.G. Császár, L. Daumont, R.R. Gamache, J.T. Hodges, O.V. Naumenko, O.L. Polyansky, L.S. Rothman, A.C. Vandaele, N.F. Zobov, A database of water transitions from experiment and theory (IUPAC Technical Report), *Pure Appl. Chem.* 86 (2014) 71-83.

- [16] J. Tauc, Optical properties and electronic structure of amorphous Ge and Si, *Mater. Res. Bull.* 3 (1967) 37-46.
- [17] F. Urbach, The long-wavelength edge of photographic sensitivity and of the electronic absorption of solids, *Phys. Rev.* 92 (1953) 1324-1329.
- [18] S. John, C. Soukoulis, M.H. Cohen, E.N. Economou, Theory of Electron Band Tails and the Urbach Optical-Absorption Edge, *Phys. Rev. Lett.* 57 (1986) 1777-1780.
- [19] R. Kink, T. Avarma, V. Kisand, A. Lohmus, I. Kink, I. Martinson, Luminescence of cation excitons in PbCl_2 and PbBr_2 crystals in a wide excitation VUV region, *J. Phys.: Condens. Matter.* 10 (1998) 693–700.
- [20] M. Iwanaga, M. Watanabe, T. Hayashi, Charge separation of excitons and the radiative recombination process in PbBr_2 crystals, *Phys. Rev. B* 62 (2000) 10766-10773.
- [21] I.N. Ogorodnikov, V.A. Pustovarov, S.I. Omelkov, L.I. Isaenko, A.P. Yelisseyev, A.A. Goloshumova, S.I. Lobanov, A far ultraviolet spectroscopic study of the reflectance, luminescence and electronic properties of SrMgF_4 single crystals, *J. Lumin.* 145 (2014) 872-879.
- [22] A.P. Yelisseyev, X. Jiang, L.I. Isaenko, L. Kang, B. Lei, Z. Lin, A.A. Goloshumova, S.I. Lobanov, D.Y. Naumov, Structures and optical properties of two phases of SrMgF_4 , *Phys. Chem. Chem. Phys.* 17 (2015) 500-508.
- [23] V.A. Pustovarov, I.N. Ogorodnikov, A.A. Goloshumova, L.I. Isaenko, A.P. Yelisseyev, A luminescence spectroscopy study of scintillation crystals SrI_2 doped with Eu^{2+} , *Opt. Mater.* 34 (2012) 926-930.
- [24] N.J. Cherepy, B.W. Sturm, O.B. Drury, T.A. Hurst, S.A. Sheets, L.E. Ahle, C.K. Saw, M.A. Pearson, S.A. Payne, A. Burger, L.A. Boatner, J.O. Ramey, E.V. van Loef, J. Glodo, R.

Hawrami, W.M. Higgins, K.S. Shah, W.W. Moses, Performance of Europium-Doped Strontium Iodide, Transparent Ceramics and Bismuth-loaded Polymer Scintillators, Proc. SPIE. 7449 (2009) 74490F.

[25] K.S. Kim, T.J. O'Leary, N. Winograd, X-Ray Photoelectron Spectra of Lead Oxides, *Analyt. Chem.* 45 (1973) 2214 – 2218.

[26] J.M. Thomas, M.J. Tricker, Electronic structure of the oxides of lead. Part 2.—An XPS study of bulk rhombic PbO, tetragonal PbO, β -PbO₂ and Pb₃O₄, *J. Chem. Soc., Faraday Trans.* 71 (1975) 329-336.

[27] S. Rondon, P.M.A. Sherwood, Core Level and Valence Band Spectra of PbO by XPS, *Surf. Sci. Spectra* 5 (1998) 97.

[28] N.M. Denysyuk, V.L. Bekenev, M.V. Karpets, O.V. Parasyuk, S.P. Danylchuk, O.Y. Khyzhun, Electronic structure of the high-temperature tetragonal Tl₃PbBr₅ phase, *J. Alloys Compd.* 576 (2013) 271–278.

[29] A. Meisel, G. Leonhardt, R. Szargan, *X-Ray Spectra and Chemical Binding*, Springer-Verlag, Berlin/Heidelberg, 1989.

Figure captions

Fig. 1. Strontium bromine plumbite crystals. An arrow points at turbid blocks.

Fig. 2. XRD pattern of middle and end parts of crystal boule, calculated one of SrPb_3Br_8 single crystal, standard one of PbBr_2 . \blacklozenge - unidentified phase.

Fig. 3. SrPb_3Br_8 crystal structure.

Fig. 4. Coordination of Pb^{2+} (a) and Sr^{2+} (b) ions in SrPb_3Br_8 structure and Pb^{2+} ions in PbBr_2 structure (c).

Fig. 5. Transmission spectra for SrPb_3Br_8 (1) and PbBr_2 (2) plates, 300 and 60 μm thick, respectively.

Fig. 6. Absorption spectra for SrPb_3Br_8 (1) and PbBr_2 (2) plates, 300 and 60 μm thick, respectively, near the absorption edge.

Fig. 7. Survey XPS spectra recorded for (1) pristine and (2) Ar^+ ion-bombarded surface of SrPb_3Br_8 crystal.

Fig. 8. Detailed XPS (a) Pb 4f, (b) Br 3p and (c) Sr $3p_{3/2}$ core-level spectra recorded for (1) pristine and (2) Ar^+ ion-bombarded surface of SrPb_3Br_8 crystal.

Fig. 9. Detailed XPS valence-band spectra recorded for (1) pristine and (2) Ar^+ ion-bombarded surface of SrPb_3Br_8 crystal.

Fig. 10. Comparison on a common energy scale of the XPS valence-band spectrum and the X-ray emission Br $K\beta_2$ band of SrPb_3Br_8 crystal.

Table 1. Crystal data and structure refinement for SrPb₃Br₈ and PbBr₂.

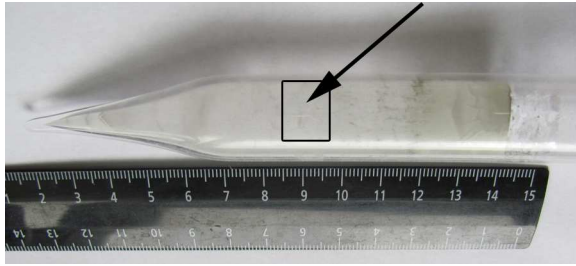
Empirical formula	Sr Pb ₃ Br ₈	Pb Br ₂
Formula weight	1356.84	367.01
Wavelength, Å	0.71073	0.71073
Crystal system	Orthorhombic	Orthorhombic
Space group	P n m a	P n m a
Unit cell dimensions	a = 8.0056(4) Å α = 90°. b = 4.7359(2) Å β = 90°. c = 9.5208(5) Å γ = 90°.	a = 8.0256(4) Å α = 90°. b = 4.7103(3) Å β = 90°. c = 9.5398(5) Å γ = 90°.
Volume, Å ³	360.97(3)	360.63(3)
Z	1	4
Density (calculated), g/cm ³	6.242	6.760
Sample size, mm ³	0.19 x 0.14 x 0.12	0.18 x 0.10 x 0.08
Theta range for data collection	from 3.32 to 28.26°	from 3.32 to 28.27°
Reflections collected	2217	2395
Independent reflections	504 [R(int) = 0.0471]	504 [R(int) = 0.0351]
Refinement method	Full-matrix least-squares on F ²	
Goodness-of-fit on F ²	1.177	1.187
Final R indices [I>2sigma(I)]	R1=0.0298, wR2=0.0798	R1=0.0224, wR2=0.0576
R indices (all data)	R1=0.0310, wR2=0.0804	R1=0.0227, wR2=0.0577

Table 2. Interatomic distances in SrPb₃Br₈ and PbBr₂.

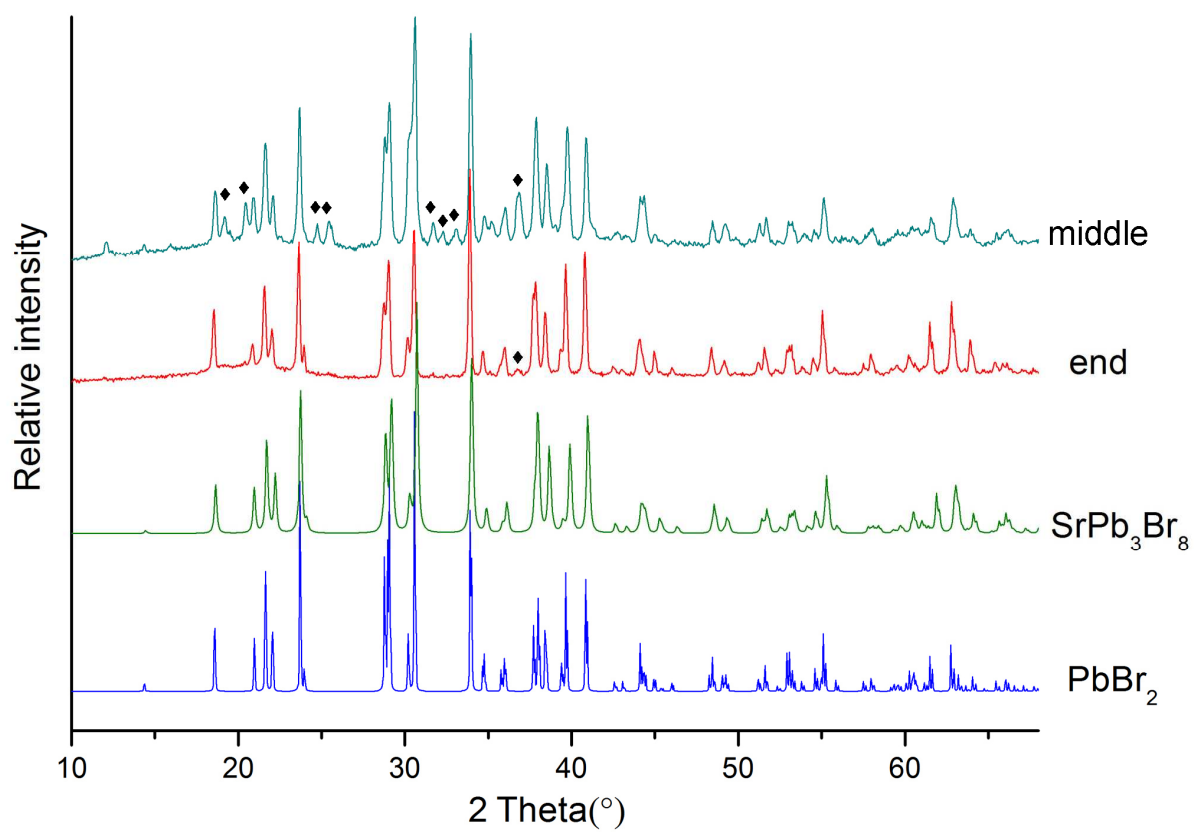
SrPb ₃ Br ₈		PbBr ₂
Sr-Br	Pb-Br	Pb-Br
3.049	2.939	2.942
3.116	3.013	3.008
3.116	3.013	3.008
3.146	3.194	3.190
3.243	3.194	3.190
3.244	3.268	3.269
3.244	3.276	3.274
3.660	3.894	3.896
3.660	3.894	3.896

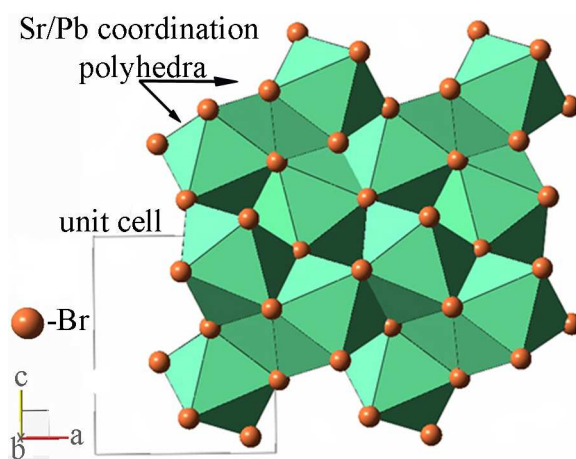
Table 3. The interpretation of absorption bands in SrPb₃Br₈.

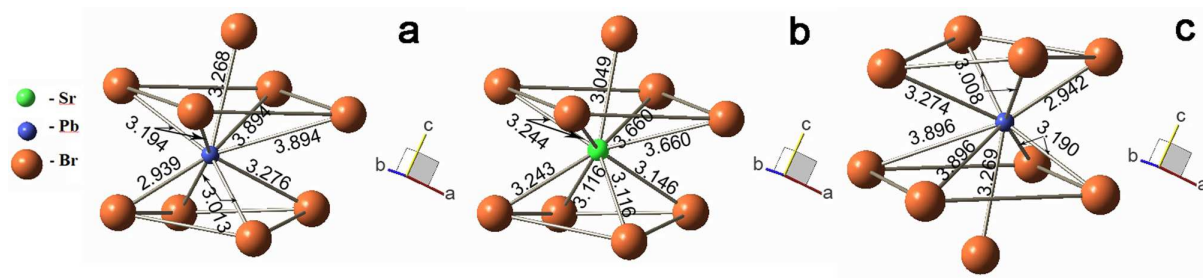
№	Wave-length, μm	Wave-number, cm^{-1}	Interpretation
1	2.89	3460	H ₂ O, ν_3 , asymmetric stretch O-H group stretch
2	6.26	1597	H ₂ O, ν_2 , bend
3	15	666	H ₂ O, L ₂ librations

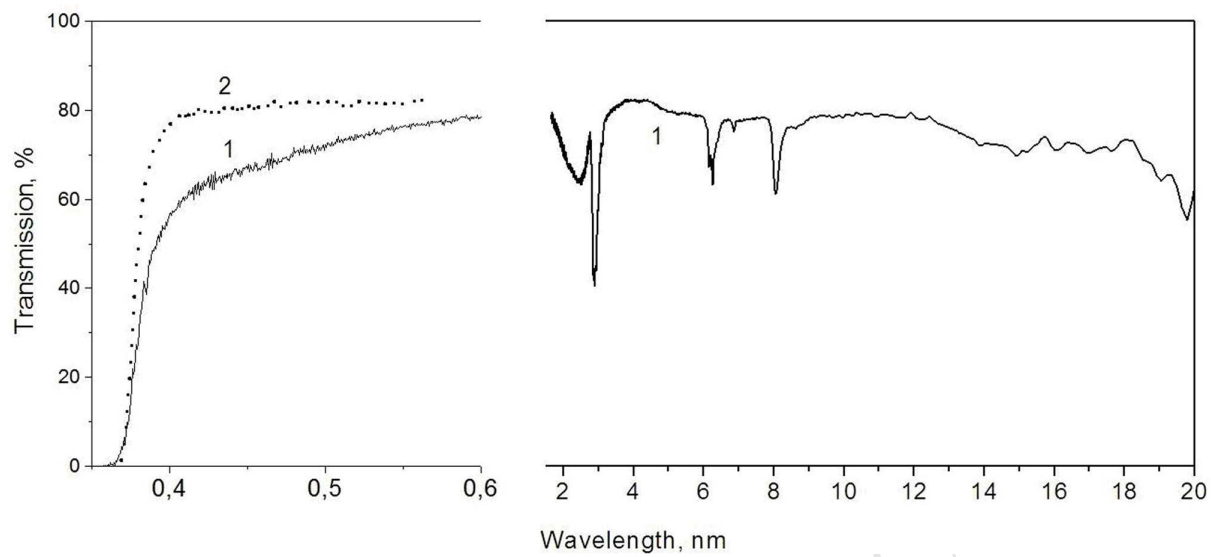


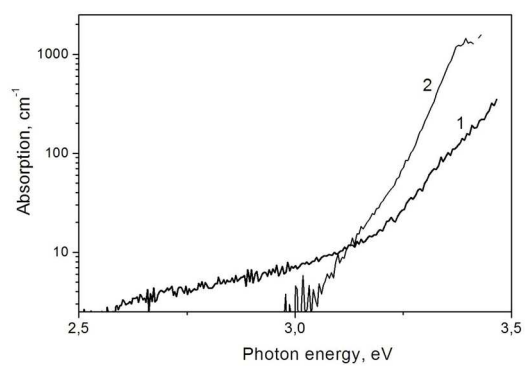
ACCEPTED MANUSCRIPT



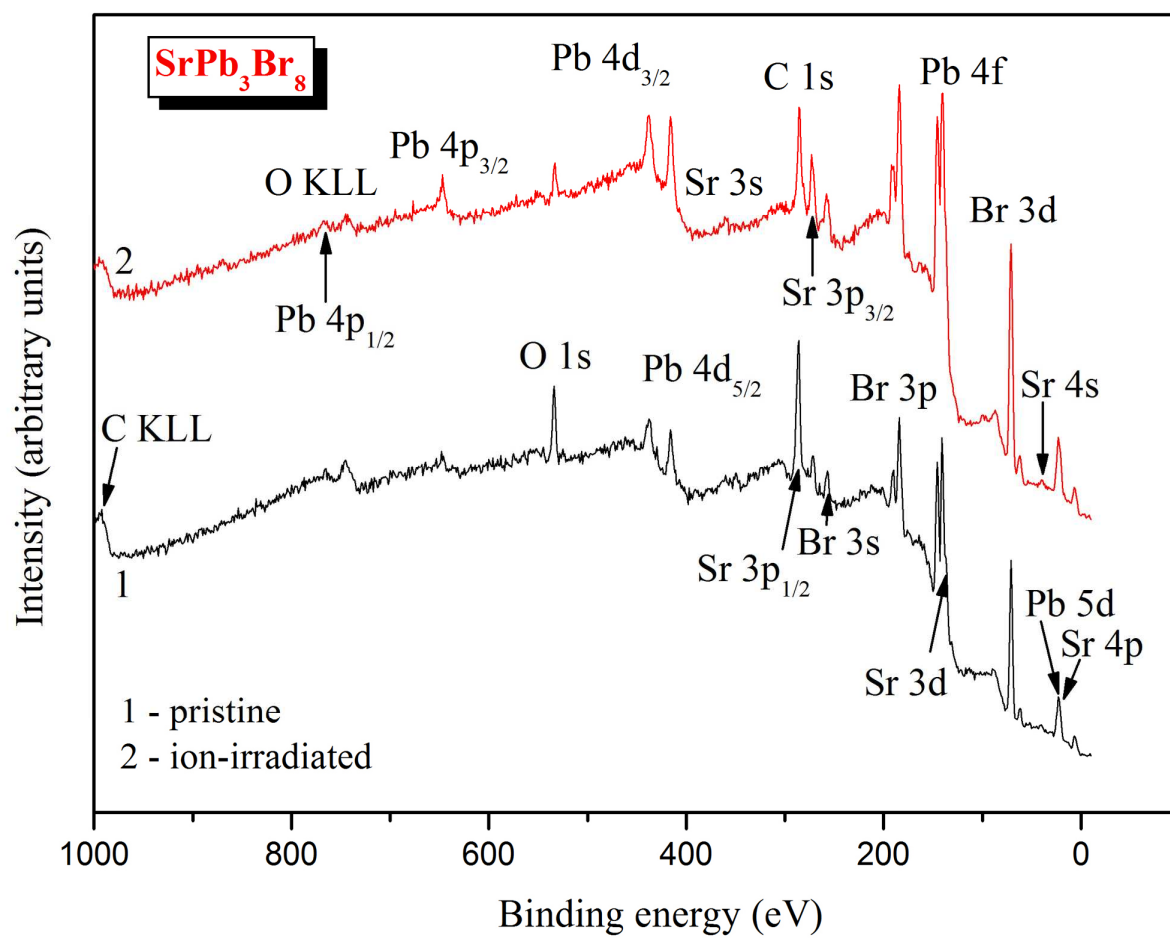


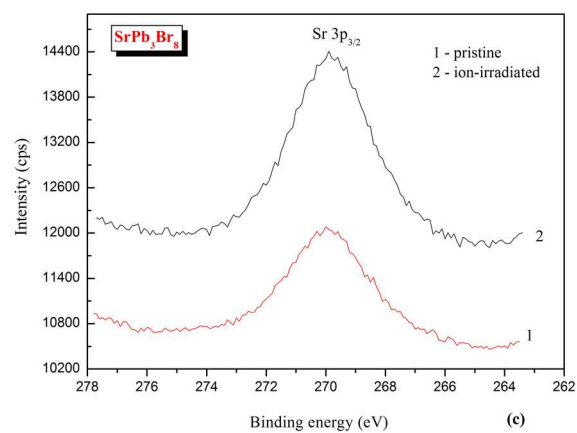
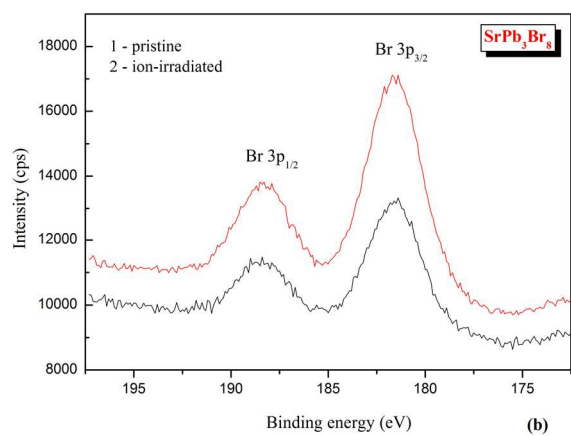
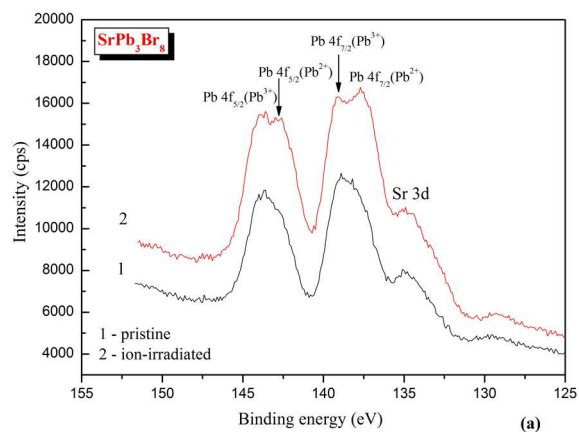


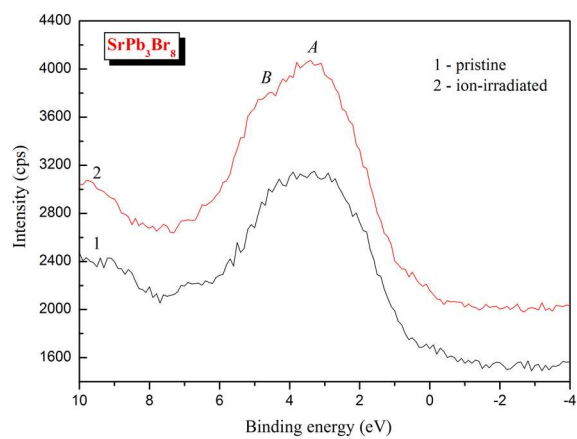


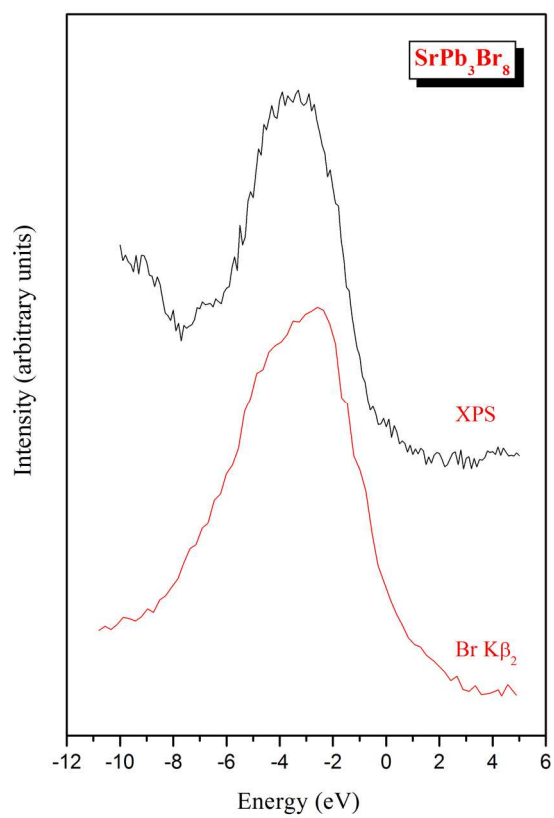


ACCEPTED MANUSCRIPT









- SrBr_2 - PbBr_2 system was investigated.
- New compound of SrPb_3Br_8 was obtained and studied by XRD and spectroscopic methods.
- Crystals have Pnma space group and are transparent from 360 nm, E_g is 3.20 eV.

ACCEPTED MANUSCRIPT